Research on Forward Position Solutions of Triangular Platform Stewart-Type Parallel Robot

LI Sa¹, YOU Jingjing^{1,2*}, WEN Wanghu¹, HUANG Ningning¹, LI Chenggang³

- 1. College of Mechanical and Electronic Engineering, Nanjing Forestry University, Nanjing 210037, P. R. China;
 - $2.\ State\ Key\ Laboratory\ of\ Mechanical\ Transmission\ for\ Advanced\ Equipment\ ,\ Chongqing\ University\ ,$

Chongqing 400044, P. R. China;

 School of Mechanical and Electrical Engineering, Nanjing University of Aeronautics and Astronautics, Nanjing 210016, P. R. China

(Received 20 June 2025; revised 30 August 2025; accepted 10 September 2025)

Abstract: This study presents a novel analytical algorithm for solving the forward position problem of a triangular platform Stewart-type parallel robot (STPR). By introducing a virtual chain and leveraging tetrahedral geometric principles, the proposed method derives analytical solutions for the position and orientation of the moving platform. The algorithm systematically addresses the nonlinearity inherent in the kinematic equations of parallel mechanisms, providing explicit expressions for the coordinates of key moving attachment points. Furthermore, the methodology is extended to general triangular platform STPRs with non-coplanar fixed attachments. Numerical validation through virtual experiments confirms the accuracy of the solutions, demonstrating that the mechanism admits eight distinct configurations for a given set of limb lengths. The results align with established kinematic principles and offer a computationally efficient alternative to iterative analytical approaches, contributing to the advancement of precision control in parallel robotic systems.

Key words: parallel robot; forward position solution; tetrahedron; analytical solution

CLC number: TH112 **Document code:** A **Article ID:** 1005-1120(2025)S-0131-10

0 Introduction

The earliest parallel robot emerged in the 1930s when Gwinnett proposed a spherical parallel mechanism for entertainment applications^[1]. A landmark theoretical study in parallel robotics was conducted by Stewart in 1965^[2], which attracted substantial academic attention and established Stewart's pioneering status in this field. Since then, Stewart-type parallel robots (STPRs) have become a predominant research focus worldwide. These robots have gained particular prominence due to their exceptional stiffness, remarkable load-bearing capacity, and minimal error accumulation^[3]. STPRs have found extensive applications in parallel kinematic

machines^[4], medical instrumentation^[5], and six-ax-is accelerometers^[6]. Furthermore, specialized configurations of parallel robots can be optimally designed to fulfill diverse operational requirements^[7-9].

From a structural topology perspective, STPRs can be classified into two primary configurations: The platform-type and the in-parallel robots. The in-parallel robot exhibits a distinct structural advantage over the platform-type configuration, as its attachment points on both the moving and fixed platforms can be spatially distributed in arbitrary three-dimensional arrangements without being constrained to a common plane.

The "100 Interdisciplinary Scientific Challenges in the 21st Century" explicitly identifies the for-

How to cite this article: LI Sa, YOU Jingjing, WEN Wanghu, et al. Research on forward position solutions of triangular platform Stewart-type parallel robot[J]. Transactions of Nanjing University of Aeronautics and Astronautics, 2025, 42(S): 131-140.

^{*}Corresponding author, E-mail address: youjingjing 251010@126.com.

ward position solution problem (also known as the direct kinematics problem) of STPRs as one of the most fundamental challenges in mechanism science. This problem is widely recognized as the "Mount Everest" of parallel robotics research and remains a critical focus for scholars. Research on forward position solutions contributes significantly to addressing key robotic performance metrics such as operational accuracy and efficiency.

Current methods for solving forward position solutions of parallel robots can be primarily categorized into two classes: Numerical methods and analytical methods^[10-11]. Numerical approaches typically employ iterative approximation techniques such as Newton-Raphson or quasi-Newton methods. Analytical methods rely on various elimination techniques to ultimately reduce the forward position solutions problem to a univariate high-order polynomial equation[12-13]. However, not all in-parallel six-degree-of-freedom (6-DoF) parallel robots possess analytical solutions. Even for those configurations that do admit analytical solutions, the derivation processes are often prohibitively complex, requiring sophisticated mathematical techniques that hinder algorithmic generalization. Furthermore, the resulting univariate polynomial equations typically remain of high degree, necessitating numerical methods for final resolution: A process that inevitably impacts computational precision and stability[14-15].

The forward position solution algorithm proposed in this work introduces a virtual kinematic chain to the parallel robot architecture. Based on tetrahedral geometry principles, this approach enables complete determination of all possible position solutions. A comprehensive literature review^[16] reveals that the complex architecture of parallel robots introduces strong coupling and nonlinearity in the moving platform's positional dynamics, rendering their forward position solutions particularly challenging to obtain. Current computational approaches for these solutions demonstrate limited efficiency. Shen et al. [17] established a correlation between the forward kinematics complexity of parallel robots and their coupling indices, specifically, higher coupling degrees correspond to greater solution difficulty, while lower coupling degrees facilitate the solution process. Li et al. [18] presented a synthesized 6-DoF parallel mechanism with analytical forward position solutions. This paper conducts an in-depth investigation of its forward position solutions by exploiting the mechanism's inherent geometric constraints, through which the complete analytical expressions for the position solutions are rigorously derived.

1 Structural Model

The structural model of the triangular platform STPR is illustrated in Fig.1. It consists of a moving platform, a fixed platform, six driving limbs, and attachment points. The moving and fixed platforms are similar triangular platforms. A triple compound hinge is mounted at one vertex of the moving platform, while a double compound hinge is mounted at one vertex of the fixed platform. The remaining attachment points are distributed along the edges of the triangular platforms and connected to the platforms via the driving limbs. The moving platform is an isosceles right triangle with a hypotenuse of length 2n, whereas the fixed platform is an isosceles right triangle with a hypotenuse of length 4n.

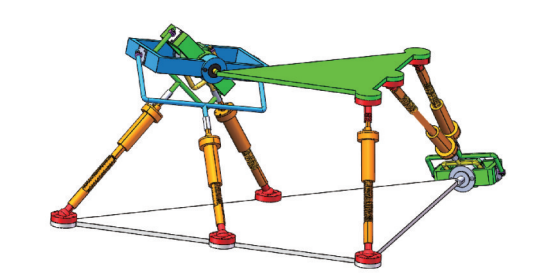


Fig.1 Structural model of the triangular platform STPR

As illustrated in Fig.2, a double-compound hinge is proposed to mitigate kinematic coupling effects. The hinge comprises two concentrically nested joint assemblies:

- (1) Outermost joint assembly. Structural elements include primary cylindrical housing, radial fork, and Type- $\rm I$ U-link.
- (2) Innermost joint assembly. Structural elements include tertiary cylindrical housing and central fork.

All assemblies feature three orthogonal revo-

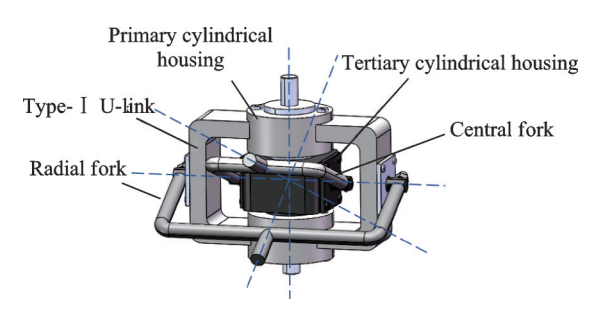


Fig.2 Double-compound hinge

lute axes that concurrently intersect at a fixed spatial point.

As illustrated in Fig.3, a triple-compound hinge is proposed to mitigate kinematic coupling effects. The hinge comprises three concentrically nested joint assemblies:

- (1) Outermost joint assembly. Structural elements include primary cylindrical housing, radial fork, and Type-I U-link.
- (2) Intermediate joint assembly. Structural elements include secondary cylindrical housing, axial fork, and Type-II U-link.
- (3) Innermost joint assembly. Structural elements include tertiary cylindrical housing and central fork.

All assemblies feature three orthogonal revolute axes that concurrently intersect at a fixed spatial point.

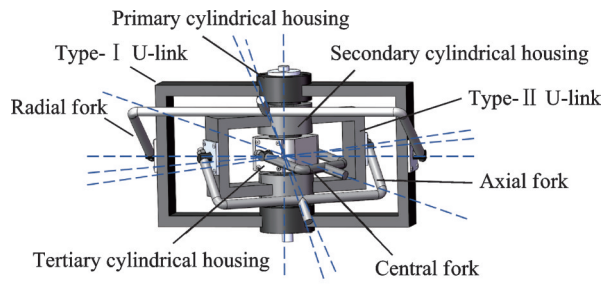


Fig.3 Triple-compound hinge

2 Positive Solution Algorithm

In spatial geometry, tetrahedron positioning can be achieved through distance constraints: Given the coordinates of three vertices, the spatial position of the fourth vertex can be uniquely determined by establishing equation systems using explicit pairwise distance relationships. Specifically, the fourth vertex coordinates are constrained by three distance equations, and solving this equation system yields

either a unique solution or symmetric solutions. This fundamental principle can be extended to the kinematic analysis of parallel robots. When provided with the robot's structural parameters and the limb lengths, which are functionally equivalent to tetrahedral edge length constraints, the spatial positions of moving attachment points (geometrically analogous to the fourth vertex of a tetrahedron) can be precisely determined through analytical solutions.

Therefore, this paper proposes a novel and efficient forward kinematics solution method. Based on the tetrahedral principle, only a virtual limb needs to be introduced to obtain all analytical-form position solutions of the parallel robot. The solution procedure is illustrated in Fig.4.

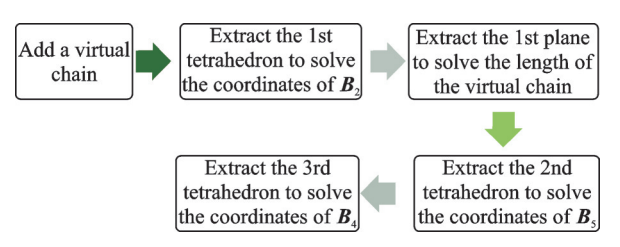


Fig.4 Flow chart of forward kinematics solution algorithm

2.1 Triangular platform STPR

The fixed coordinate frame o-xyz is established on the fixed platform, with its origin located at the midpoint of the centerline along the hypotenuse of the platform. Similarly, the moving coordinate frame g-muv is defined on the moving platform, originating at the midpoint of its hypotenuse centerline, as illustrated in Fig.5.

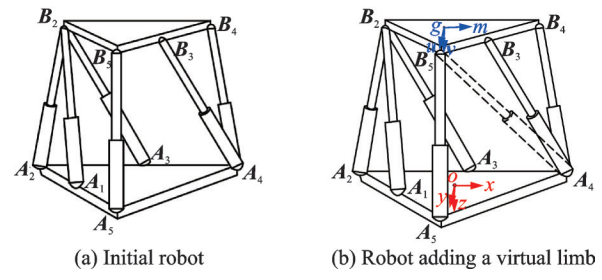


Fig.5 Sketch of the triangular platform STPR

The centers of the fixed attachment points are denoted as A_1 — A_5 , the centers of the moving attachment points are denoted as B_2 — B_5 , and the lengths of the six driving limbs are denoted as l_1 — l_6 . The coordinates of B_2 , B_5 , and B_4 are denoted as

 $(x,y,z)^{\mathrm{T}}$, $(u,v,w)^{\mathrm{T}}$, and $(r,s,t)^{\mathrm{T}}$, respectively.

Since attachment points A_1 , A_3 , and B_3 can be arbitrarily positioned on edges A_2A_5 , A_2A_4 , B_4B_5 , respectively, the lengths of A_1A_2 , A_2A_3 , and B_3B_4 can be respectively denoted as

$$\frac{|A_1 A_2|}{|A_2 A_5|} = \lambda_1, \frac{|A_2 A_3|}{|A_2 A_4|} = \lambda_2, \frac{|B_3 B_4|}{|B_4 B_5|} = \lambda_3$$

In the subsequent analysis, for computational convenience, the moving and fixed platforms are modeled as isosceles right triangles with hypotenuse lengths of 2n and 4n, respectively. Additionally, $\lambda_1 = \lambda_2 = \lambda_3 = 0.5$, indicating that the three attachment points A_1 , A_3 and B_3 are located at the midpoints of their respective edges.

The coordinates of the five fixed attachment points in o-xyz are

$$(A_1, A_2, A_3, A_4, A_5) = \begin{pmatrix} -n & -2n & 0 & 2n & 0 \\ 0 & -n & -n & -n & n \\ 0 & 0 & 0 & 0 & 0 \end{pmatrix}$$
 (1)

Extract the 1st tetrahedron B_2 - A_1 - A_2 - A_3 from Fig.5(b), as shown in Fig.6.

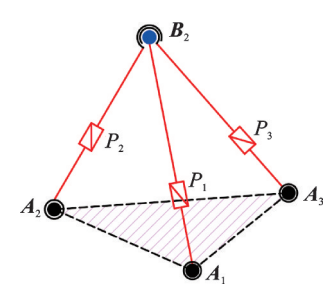


Fig.6 Schematic diagram of tetrahedron 1

There exists a system of constraint equations, shown as

$$\begin{cases} ||A_1 - B_2|| = l_1 \\ ||A_2 - B_2|| = l_2 \\ ||A_3 - B_2|| = l_3 \end{cases}$$
 (2)

where $\| \bullet \|$ denotes the paradigm of the vector.

Substitute Eq.(1) into Eq.(2) and expand as

$$\begin{cases} (x+n)^2 + y^2 + z^2 = l_1^2 \\ (x+2n)^2 + (y+n)^2 + z^2 = l_2^2 \\ x^2 + (y+n)^2 + z^2 = l_3^2 \end{cases}$$
 (3)

Solving Eq.(3) yields the coordinates of B_2 , shown as

$$\begin{cases} x = \frac{l_2^2 - l_3^2}{4n} - n \\ y = \frac{-2l_1^2 + l_2^2 + l_3^2}{4n} - n \end{cases}$$

$$z = \frac{\pm \bar{b}_2}{2\sqrt{2} n}$$
(4)

where \bar{b}_2 =

$$\sqrt{2l_1^2 - l_1^2 + l_2^2 + l_3^2 - l_2^4 - l_3^4 + 4n^2(l_2^2 + l_3^2 - 2n^2)}.$$

Plane 1 $(A_4 - B_5 - B_4 - B_3)$ is extracted from Fig. 5(b), as shown in Fig. 7.

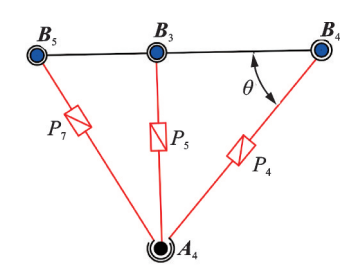


Fig.7 Schematic diagram of plane 1

There exists a relational equation. For $\Delta B_3 B_4 A_4$, it is shown as

$$\cos \theta = \frac{l_4^2 + \frac{1}{2}n^2 - l_5^2}{\sqrt{2}l_4n} \tag{5}$$

And for $\Delta B_5 B_4 A_4$, it is shown as

$$\cos \theta = \frac{l_4^2 + 2n^2 - l_7^2}{2\sqrt{2} l_4 n} \tag{6}$$

By associating Eq.(5) with Eq.(6), the length of the virtual limb A_4B_5 can be solved as

$$l_7 = \sqrt{n^2 - l_4^2 + 2l_5^2} \tag{7}$$

The 2nd tetrahedron(B_5 - B_2 - A_5 - A_4) is extracted from Fig.5(b), as shown in Fig.8.

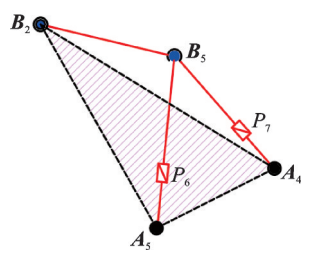


Fig.8 Schematic diagram of tetrahedron 2

There exists a system of constraint equations, shown as

$$\begin{cases} \|B_{5} - B_{2}\| = \sqrt{2} n \\ \|B_{5} - A_{5}\| = l_{6} \\ \|B_{5} - A_{4}\| = l_{7} \end{cases}$$
 (8)

Substitute Eq.(1) into Eq.(8) and expand as

$$\begin{cases} (u-x)^{2} + (v-y)^{2} + (w-z)^{2} = 2n^{2} \\ u^{2} + (v-n)^{2} + w^{2} = l_{6}^{2} \\ (u-2n)^{2} + (v+n)^{2} + w^{2} = l_{7}^{2} \end{cases}$$
(9)

Solving Eq.(9) yields the coordinates of B_5 , shown as

$$\begin{cases} u = \frac{-b_1 c_1 + d_1 \pm \bar{D}_2}{\bar{D}_1} \\ v = \frac{b_1 c_2 + d_2 \pm \bar{D}_2}{\bar{D}_1} \\ w = \frac{b_2 \pm \bar{D}_2 (n - x - y)}{\bar{D}_1 z} \end{cases}$$
(10)

where $\bar{D}_1 = 4n^2 \left(\left(-n + x + y \right)^2 + 2z^2 \right)$; $b_1 = n \left(n - x - y \right)$; $c_1 = l_7^2 \left(n - y \right) + l_6^2 \left(n + y \right) + 2n \left(-5n^2 + 2ny + x^2 + y^2 \right)$; $d_1 = nz^2 \left(l_6^2 - l_7^2 + 2n \left(3n + y + x \right) \right)$; $c_2 = 6n^3 - l_7^2 x + 4n^2 + l_6^2 \left(-2n + x \right) - 2n (x^2 + y^2)$; $d_2 = nz^2 \left(-l_6^2 + l_7^2 \right) + 2n \left(-n + y + x \right)$; $b_2 = -12n^4 z^2 - 8n^3 xz^2 - nz^2 \left(l_6^2 - l_7^2 \right) \left(x - y \right) + n^2 z^2 \left(3l_6^2 + l_7^2 + 4 \left(x^2 + y^2 + z^2 \right) \right)$; and \bar{D}_2 is an analytic equation on x, y, z, n, l_6 , and l_7 .

The 3rd tetrahedron $(B_2-B_4-B_5-A_4)$ is extracted

tetralieuron (
$$D_2 D_4 D_5 A_4$$
) is extracted

$$\begin{cases} r = \frac{E_1 + n^2 p_1 - np_2 \mp \bar{D}_4}{\bar{D}_3} \\ s = \frac{E_2 + n^4 p_3 + n^3 p_4 + n^2 p_5 \pm \bar{D}_4 (-2nw + wx + 2nz - uz)}{\bar{D}_3} \\ t = \frac{E_3 + n^3 p_6 + n^2 p_7 + n^4 p_8 + np_9 \pm \bar{D}_4 (nu + 2nv - nx - vx - 2ny + uy)}{\bar{D}_3} \end{cases}$$

$$(13)$$

where \bar{D}_3 =2 $(u^2y^2+w^2(x^2+y^2)+n^2((u+2v-x-2y)^2+5(w-z)^2)-2uwxz+u^2z^2-2vy(ux+wz)+v^2(x^2+z^2)+2n(-2v^2x+u^2y-w(2x-y)+w(w-z)+v(x^2+2xy-wz+z^2)-u(v(x-2y)+y(x+2y)+2z(-w+z))$; p_3 = $-w(9u^2+9w^2+2u(9v-8x-13y)-2v(5x+4y)+(x+2y)(7x+4y)$)+ $z(9u^2-8v^2+25w^2+2u(7v-8x-11y)+7x(x+2y)+v(-6x+8y))-23wz^2+7z^3$; p_8 =(w-z)(9vw+5w(2x+y)+7z(-3v-2x+y)+u(-18w+22z); \bar{D}_4 , E_1 , E_2 , E_3 are analytic equations with respect to u, v, w, x, y, z, l_4 , and n; and p_1 , p_2 , p_4 , p_5 , p_6 , p_7 , p_9 are analytic equations with respect to u, v, w, x, y, z, and n.

The fixed coordinate frame and the moving platform are extracted from Fig.5, as shown in Fig.10.

from Fig.5(b), as shown in Fig.9.

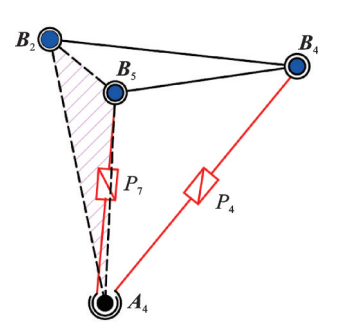


Fig.9 Schematic diagram of tetrahedron 3

There exists a system of constraint equations, shown as

$$\begin{cases} \|B_4 - A_4\| = l_4 \\ \|B_4 - B_2\| = 2n \\ \|B_4 - B_5\| = \sqrt{2} n \end{cases}$$
 (11)

Substitute Eq.(1) into Eq.(11) and expand as

$$\begin{cases} (r-2n)^{2} + (s+n)^{2} + t^{2} = l_{4}^{2} \\ (r-x)^{2} + (s-y)^{2} + (t-z)^{2} = 4n^{2} \\ (r-u)^{2} + (s-v)^{2} + (t-w)^{2} = 2n^{2} \end{cases}$$
(12)

Solving Eq.(12) yields the coordinates of B_4 , shown as

$$B_2$$
 B_3
 B_3
 B_4
 B_5
 P_1
 P_2
 P_2
 P_3
 P_4
 P_2
 P_3
 P_4
 P_2
 P_3
 P_4
 P_2
 P_4
 P_2
 P_4
 P_5
 P_5

Fig.10 Partial schematic diagram of moving platform

The coordinates of g in the fixed coordinate frame can be found from the positional relationship between B_2 , B_4 , and B_5 on the moving platform, shown as

$$g = \frac{1}{4} (B_2 + B_4) + \frac{1}{2} B_5 \tag{14}$$

Within the moving coordinate frame, B_3 is posi-

tioned at the terminus of the m-axis, B_5 lies at the extremity of the u-axis, and point g coincides with the frame origin. The coordinates of B_3 , B_5 , and g in the fixed coordinate frame o-xyz are $B_3 = \left(\frac{u+r}{2}, \frac{v+s}{2}, \frac{w+t}{2}\right)^{\mathsf{T}}$, $g = (x_1, y_1, z_1)$, $B_5 =$

 $(u, v, w)^{\mathsf{T}}$, and the corresponding vectors for the *m*-axis, *u*-axis, and *v*-axis of the moving platform's coordinate frame g-muv are denoted as $\alpha = (\alpha_x, \alpha_y, \alpha_z)^{\mathsf{T}}$, $\beta = (\beta_x, \beta_y, \beta_z)^{\mathsf{T}}$, and $\gamma = (\gamma_x, \gamma_y, \gamma_z)^{\mathsf{T}}$.

Then, α , β , and γ are obtained after expressing them in terms of the coordinates of the points B_3 , B_5 , and g, shown as

$$\alpha = B_3 - g \tag{15}$$

$$\beta = B_5 - g \tag{16}$$

$$\gamma = \alpha \times \beta \tag{17}$$

So, the rotation matrix R of g-muv with respect to o-xyz can be expressed as

$$R = \begin{bmatrix} \alpha & \beta & \gamma \end{bmatrix} = \begin{bmatrix} \alpha_x & \beta_x & \gamma_x \\ \alpha_y & \beta_y & \gamma_y \\ \alpha_z & \beta_z & \gamma_z \end{bmatrix}$$
(18)

2. 2 General triangular platform STPR

In the following content, the proposed method is extended to the general triangular platform STPRs where the fixed attachment points on the fixed platform are non-coplanar, as shown in Fig.11.

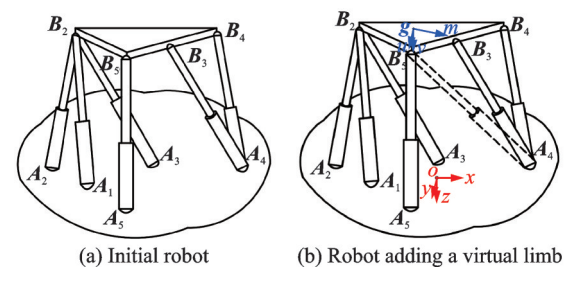


Fig.11 Sketch of the general triangular platform STPR

The coordinates of the five fixed attachment points in o-xyz are

$$(A_{1}, A_{2}, A_{3}, A_{4}, A_{5}) = \begin{pmatrix} -n & -2n & 0 & 2n & 0\\ 0 & -n & -n & -n & n\\ 0 & -0.1n & -0.3n & -0.4n & -0.2n \end{pmatrix} (19)$$

Extract the 1st tetrahedron B_2 - A_1 - A_2 - A_3 from Fig.11(b), substitute Eq.(19) into Eq.(2) and ex-

pand as

$$\begin{cases} (x+n)^2 + y^2 + z^2 = l_1^2 \\ (x+2n)^2 + (y+n)^2 + (z+0.1n)^2 = l_2^2 (20) \\ x^2 + (y+n)^2 + (z+0.3n)^2 = l_3^2 \end{cases}$$

Plane 1 A_4 - B_5 - B_4 - B_3 is extracted from Fig.11(b), and the length of the virtual limb A_4B_5 , i.e. l_7 , can be solved by Eq.(7).

The 2nd tetrahedron B_5 - B_2 - A_5 - A_4 , extracted from Fig.11(b), substitutes Eq.(19) into Eq.(8) and can be expanded as

$$\begin{cases} (u-x)^{2} + (v-y)^{2} + (w-z)^{2} = 2n^{2} \\ u^{2} + (v-n)^{2} + (w+0.2n)^{2} = l_{6}^{2} \\ (u-2n)^{2} + (v+n)^{2} + (w+0.4n)^{2} = l_{7}^{2} \end{cases}$$
(21)

The 3rd tetrahedron B_2 - B_4 - B_5 - A_4 , extracted from Fig.11(b), substitutes Eq.(19) into Eq.(11) and can be expanded as

$$\begin{cases} (r-2n)^{2} + (s+n)^{2} + (t+0.4n)^{2} = l_{4}^{2} \\ (r-x)^{2} + (s-y)^{2} + (t-z)^{2} = 4n^{2} \\ (r-u)^{2} + (s-v)^{2} + (t-w)^{2} = 2n^{2} \end{cases}$$
 (22)

3 Algorithm Validation

The pose of the moving platform is defined by the Cartesian coordinates of its centroid (point g) in the fixed reference frame, along with its orientation represented by ZYX Euler angles $[\alpha, \beta, \gamma]$, where α, β , and γ correspond to rotations about the local X^- , Y^- , and Z^- axes, respectively.

A virtual prototype of the triangular Stewarttype parallel mechanism is developed, as illustrated in Fig.12. The moving platform has a hypotenuse measuring 30 mm in length. For any specified set of six driving limb lengths, the simulation enables simultaneous measurement of both the position of the platform centroid and the orientation Euler angles.

Following the methodology described in Section 2, the coordinates of centroid g and the orientation Euler angles of the moving platform can be computationally determined and validated against simulation-measured data (Figs.13 and 14). The comparative analysis demonstrates excellent agreement between the calculated and simulated values, confirming the accuracy of the algorithm.

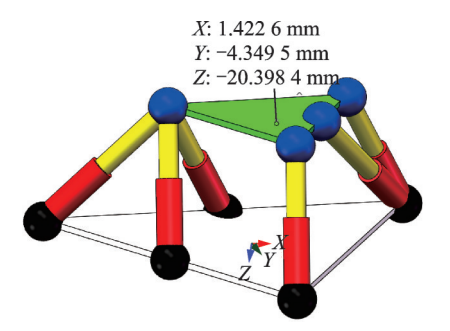


Fig.12 Virtual prototype of the triangular platform STPR

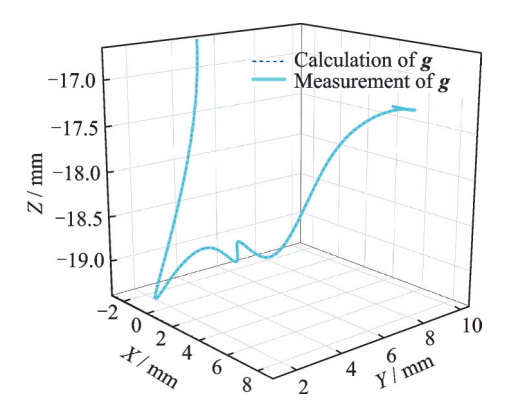


Fig.13 Verification examples of position coordinates of the g-point

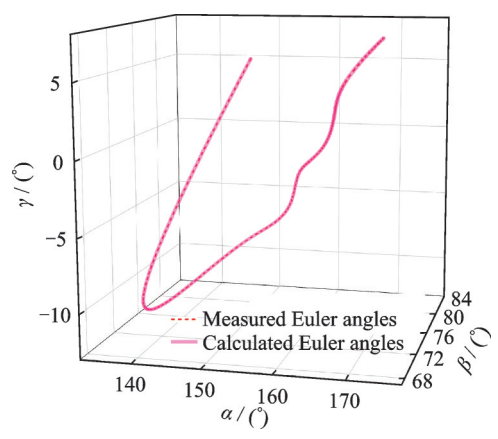


Fig.14 Verification examples of Euler angles of the moving platform

Using the same method, a virtual prototype of the general triangular-platform STPR is shown in Fig.15, and verification examples of position coordinates for point g and Euler angles for the moving platform are shown in Figs.16 and 17.

4 Multiple Solutions

The presence of " \pm " signs in Eqs.(4,10,13) indicates that multiple sets of forward position solutions exist for a given set of input limb lengths in the parallel robot. Therefore, the triangular platform

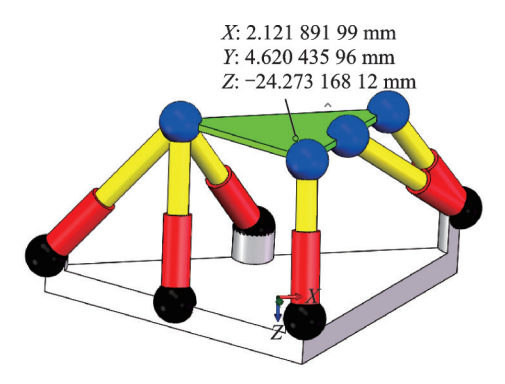


Fig.15 Virtual prototype of the general triangular platform STPR

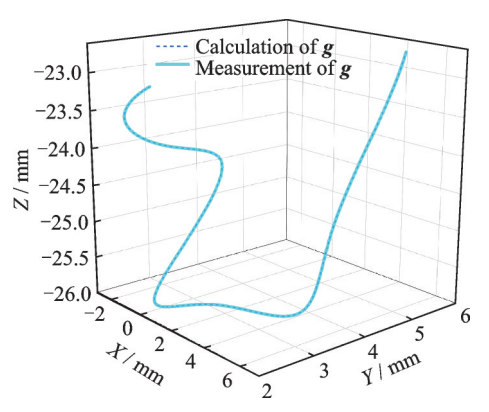


Fig.16 Verification examples of position coordinates of the g-point of the general triangular platform STPR

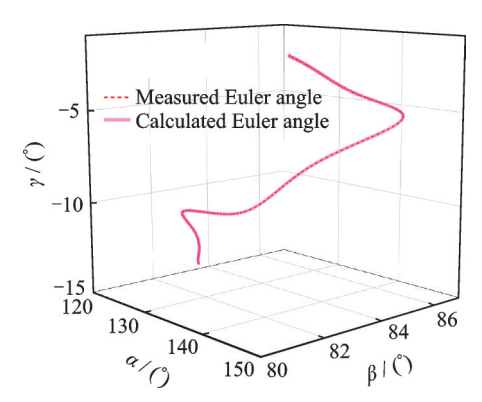


Fig.17 Verification examples of Euler angles of the moving platform of the general triangular platform STPR

STPR and the general triangular platform STPR generally possess eight distinct forward position solution configurations, as detailed in Tables 1 and 2. The corresponding schematic diagrams of these mechanisms are presented in Tables 3 and 4, respectively. Notably, the eight solution sets of the triangular-platform STPR form four symmetric pairs about the *XOY* plane, with each pair distributed bilaterally across this reference plane.

Table 1	Solution multipli	city of forward	position solutions	for triangular	platform STPR

Group	$B_2(x, y, z)$	$B_{\scriptscriptstyle 5}\left(u,v,w ight)$	$B_4(r, s, t)$	
1		(12 121 5 7 500 0 0 020 7)	(1.5548, -22.6433, -2.3867)	
2	(-15.6166, -6.6504, -21.0782)	(-13.1215, -7.5088, -0.0297)	$(5.813\ 3,\ 1.872\ 3,\ -1.891\ 7)$	
3		$(0.759\ 9,\ 6.372\ 6,\ -24.572\ 6)$	$(7.362\ 3,\ 3.421\ 2,\ -4.630\ 2)$	
4			(13.9891, -10.2090, -24.3709)	
5	(15 010 0	(-13.121 5, -7.508 8, 0.029 7)	$(1.554\ 8,\ -22.643\ 3,\ 2.386\ 7)$	
6			(5.813 3, 1.872 3, 1.891 7)	
7	(-15.6166, -6.6504, 21.0782)	(0.750.0. 0.279.0. 24.579.0)	(7.362 3, 3.421 2, 4.630 2)	
8		(0.759 9, 6.372 6, 24.572 6)	(13.9891, -10.2090, 24.3709)	

Table 2 Solution multiplicity of forward position solutions for the general triangular platform STPR

Group	$B_2(x, y, z)$	$B_{\scriptscriptstyle 5}\left(u,v,w ight)$	$B_4\left(r,s,t ight)$	
1		(-9.8795, -1.7030, 4.02492)	(1.3600, -17.6919, -4.2173)	
2	(-10.4221, -11.7183, 22.7171)	(-9.879.5, -1.703.0, 4.024.92)	$(10.777\ 4,\ 2.275\ 9,\ 6.756\ 44)$	
3		(-1.1073, 5.9216, 15.5014)	(3.5770, -3.9825, -2.6636)	
4		(-1.107 5, 5.921 6, 15.501 4)	(17.8871, -3.3299, 17.4047)	
5		(-11.2588, -2.1736, -5.0624)	(1.4953, -18.9229, -7.6686)	
6	(15 202 0 1 007 0 25 000 7)		(8.6367, 4.1354, -8.8529)	
7	(-15.2828, -1.9970, -25.8897)	(0.740.111.669.2	(6.4713, 1.6400, -5.5542)	
8		(0.7481, 11.6623, -23.3530)	(14.6107, -3.8096, -27.6480)	

Table 3 Schematic diagrams of mechanism configuration for the triangular platform STPR

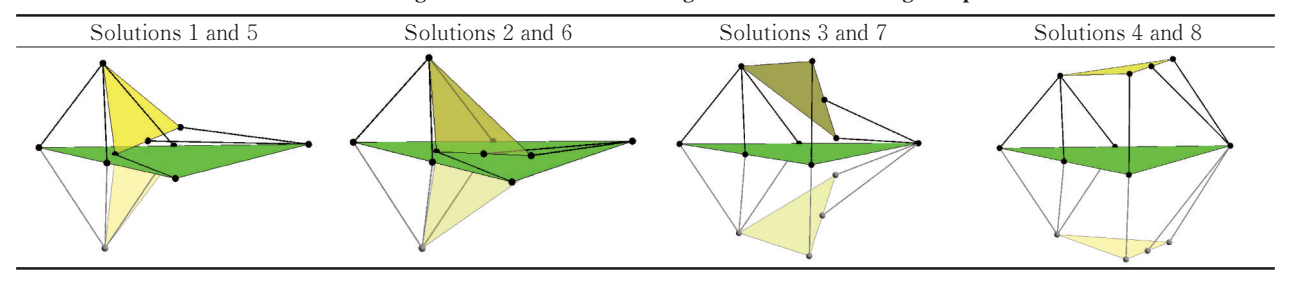
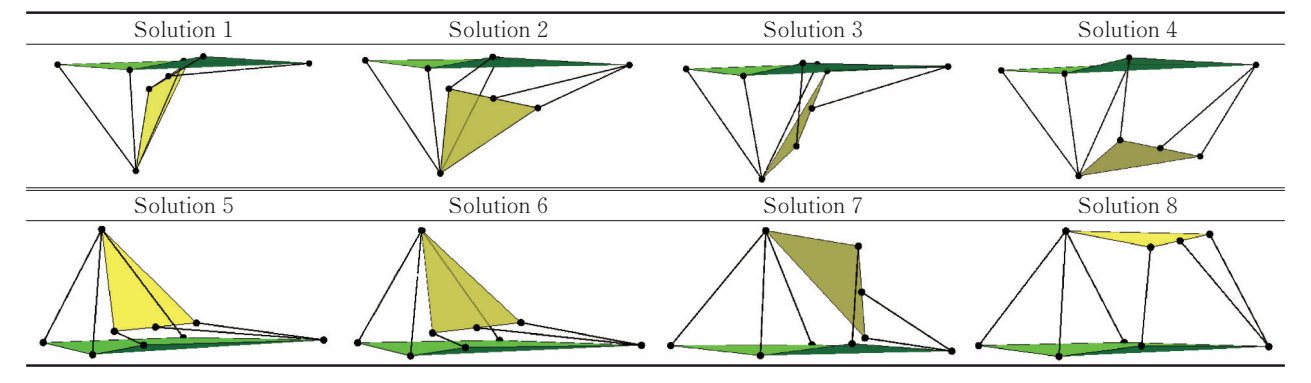


Table 4 Schematic diagrams of mechanism configuration for the general triangular platform STPR



5 Conclusions

(1) This study proposes a novel analytical algorithm for the forward position solution of a triangular platform STPR. The method introduces a virtual chain and employs tetrahedral geometry principles to derive explicit expressions for the moving

platform's position and orientation.

- (2) The algorithm is generalized to accommodate non-coplanar fixed attachment points, extending its applicability to a broader class of triangular platform STPRs.
- (3) Numerical validation using virtual prototypes confirms the accuracy of the derived solu-

tions, with the mechanism exhibiting eight distinct forward position configurations for a given set of limb lengths. These results are consistent with theoretical expectations.

(4) The study contributes to the field by providing a computationally efficient and geometrically intuitive approach to the forward kinematics problem, offering potential benefits for real-time control and precision applications in parallel robotics.

References

- [1] GWINNETT J E. Amusement device: US1789680 [P]. 1931-01-20.
- [2] STEWART D. A platform with six degrees of free-dom[J]. Proceedings of the Institution of Mechanical Engineers, 1965, 180(15): 371-386.
- [3] WANG Shusheng, YOU Jingjing, HUANG Ningning, et al. Structural design and kinematic analysis of a new reconfigurable 3-DOF planar parallel mechanism[J]. Journal of Nanjing University of Aeronautics & Astronautics, 2023, 55(3): 437-443. (in Chinese)
- [4] ZHENG Y. Research on application of parallel robot in concrete precast construct producing line[J]. Machine Tool & Hydraulic, 2018, 46(13): 104-106.
- [5] SABATE N, ESQUIVEL J P, SANTANDER J, et al. New approach for batch microfabrication of silicon-based microfuel cells[J]. Microsystem Technologies, 2014, 20(2): 341-348.
- [6] YOU Jingjing, LI Chenggang, WU Hongtao. Performance modeling structure optimizing of six-axis accelerometer[J]. Journal of Nanjing University of Aeronautics & Astronautics, 2013, 45(3): 380-389. (in Chinese)
- [7] YOU J J, YAN F, ZHOU W, et al. Research on the forward position solution of piezoelectric driven platform parallel mechanism[J]. Piezoelectrics & Acoustooptics, 2017, 39(6): 829-833.
- [8] YOU J J, XI F F, SHEN H P, et al. A novel Stewart type parallel mechanism with topological reconfiguration: Design, kinematics and stiffness evaluation[J]. Mechanism and Machine Theory, 2021, 162: 104329.
- [9] DUZQ, LIJ, MENGQM, et al. Symbolic position analysis for three 6-DOF parallel mechanisms and new insight[J]. Robotica, 2024, 42(5): 1628-1648.
- [10] LUQP, LIYJ, PENGZQ, et al. Forward kinematics of six-bar parallel mechanism and its applications in synchrotron radiation beam-line[J]. Optics and Precision Engineering, 2008, 16(10): 1874-1879.

- [11] GENG M C, ZHAO T S, WANG C, et al. Direct position analysis of parallel mechanism based on quasi-Newton method[J]. Journal of Mechanical Engineering, 2015, 51(9): 28-36.
- [12] YANG X L, LIAO Q Z, WEI S M, et al. A dual quaternion solution to the forward kinematics of a class of six-DOF parallel mechanisms with full or reductant actuation[J]. Mechanism Theory, 2017, 107: 27-36.
- [13] ZHOU W Y, CHEN W Y, LIU H D, et al. A new forward kinematics algorithm for a general Stewart platform[J]. Mechanism and Machine Theory, 2015, 87: 177-190.
- [14] LIU M Z, GU Q X, YANG B, et al. Kinematics model optimization algorithm for six degrees of freedom parallel platform[J]. Applied Sciences, 2023, 13 (5): 3082.
- [15] FENG Z Y, LI Y G, ZHANG C, et al. Current status and prospect of motion and dynamic analysis of parallel robot mechanism[J]. China Mechanical Engineering, 2006, 17(9): 979-984.
- [16] SHEN Huiping, ZHONG Rui, LI Ju, et al. Influence of different distribution order of joints on kinematic and dynamic performance of parallel mechanism[J]. Transactions of the Chinese Society for Agricultural Machinery, 2023, 54(7): 412-426. (in Chinese)
- [17] SHEN H P, YIN H B, WANG Z, et al. Research on forward position solutions for 6-SPS parallel mechanisms based on topology structure analysis[J]. Journal of Mechanical Engineering, 2013, 49(21): 70-80.
- [18] LICG, XIAYH, YOUJJ, et al. Six-degree-of-free-dom parallel mechanism with closed kinematic position solution and analytical method: CN201210457801.1 [P]. 2015-01-14.

Acknowledgements This work was supported by the Opening Project of State Key Laboratory of Mechanical Transmission for Advanced Equipment (No. SKLMT-MSKFKT-202330), the National Natural Science Foundation of China (No.52575022); and the Jiangsu Province Postgraduate Research & Practice Innovation Program (No.KYCX25_1403).

Authors

The first author Ms. LI Sa is a postgraduate student in mechanical engineering at Nanjing Forestry University. She focuses on parallel mechanisms.

The corresponding author Dr. YOU Jingjing received the B. S. degree in mechanical and electronic engineering from Nanjing Forestry University in 2007, and received the M.S. and Ph.D. degrees in mechanical and electronic engineering from Nanjing University of Aeronautics and Astronautics in 2010 and 2013, respectively. He joined in Nanjing Forestry

University in January 2014, where he is an associate professor of Machine Design Laboratory. His research is focused on parallel robots.

Author contributions Ms. LI Sa designed the study, complied the models and wrote the manuscript. Dr. YOU Jingjing contributed to data analysis, result interpretation and manuscript revision. Mr. WEN Wanghu contributed to

the discussion and revision of the study. Mr. HUANG Ningning contributed to data analysis of the study. Mr. LI Chenggang contributed to the discussion and background of the study. All authors commented on the manuscript draft and approved the submission.

Competing interests The authors declare no competing interests.

(Production Editor: ZHANG Huangqun)

三角平台式Stewart型并联机器人的位置正解研究

李 飒1, 尤晶晶1,2, 闻王虎1, 黄宁宁1, 李成刚3

(1.南京林业大学机械电子工程学院,南京 210037,中国; 2.重庆大学高端装备机械传动全国重点实验室,重庆 400044,中国; 3.南京航空航天大学机电学院,南京 210016,中国)

摘要:本文提出了一种用于求解三角平台式 Stewart 型并联机器人(Stewart-type parallel robot, STPR)位置正解问题的新型解析算法。通过引入一条虚拟链并运用四面体几何原理,该方法能够解析求解动平台的位姿参数。该算法系统地解决了并联机构运动学方程固有的非线性问题,求解出了关键动铰点坐标的显式表达式。进一步研究表明,该方法可推广应用于静铰点非共面布置的广义三角平台式 Stewart 型并联机构。虚拟仿真实验验证了本文算法的正确性,并且该机构在给定支链长度条件下存在八组不同的位形构型。研究结果符合经典运动学理论,为并联机器人系统提供了一种计算高效的解析求解新方法,对提升精密控制性能具有重要理论意义。

关键词:并联机器人;位置正解;四面体;解析解